

New Relativistic Effects in the Dynamics of Nonlinear Hydrodynamical Waves

Luciano Rezzolla^{1,2} and Olindo Zanotti¹

¹*SISSA, International School for Advanced Studies, Trieste, Via Beirut 2–4, 34014 Trieste, Italy*

²*INFN, Department of Physics, University of Trieste, Via Valerio 2, 34127 Trieste, Italy*

(November 1, 2018)

In Newtonian and relativistic hydrodynamics the Riemann problem consists of calculating the evolution of a fluid which is initially characterized by two states having different values of uniform rest-mass density, pressure and velocity. When the fluid is allowed to relax, one of three possible wave-patterns is produced, corresponding to the propagation in opposite directions of two nonlinear hydrodynamical waves. New effects emerge in a special relativistic Riemann problem when velocities tangential to the initial discontinuity surface are present. We show that a smooth transition from one wave-pattern to another can be produced by varying the initial tangential velocities while otherwise maintaining the initial states unmodified. These special relativistic effects are produced by the coupling through the relativistic Lorentz factors and do not have a Newtonian counterpart.

PACS Numbers: 47.40.N, 47.35, 47.85.D

More than a hundred years ago, Riemann addressed the problem of the one-dimensional time evolution of a perfect fluid which, at some given initial time $t = 0$, is composed of two adjacent states characterized by different values of uniform velocity, pressure and density [1]. Since then this problem has been referred to as the “Riemann problem” and is the prototype of the initial value problem for hyperbolic systems of partial differential equations with discontinuous initial conditions. The conclusion reached by Riemann in Newtonian hydrodynamics is that the one-dimensional flow that develops when the barrier separating the initial “left” (or 1) and “right” (or 2) states is removed, will allow for four different and distinct solutions. All of the solutions are composed of nonlinear waves, in the form of either shock waves or rarefaction waves, that propagate in opposite directions and join the two unperturbed left and right states. As a result, three different “wave-patterns” can be produced corresponding to two shock waves ($2S$), a shock and rarefaction wave (SR) and two rarefaction waves ($2R$), respectively. Schematically, the fluid solution for any $t > 0$ can therefore be represented as

$$1 \mathcal{W}_{\leftarrow} 3 \mathcal{C} 3' \mathcal{W}_{\rightarrow} 2, \quad (1)$$

where \mathcal{W} denotes a shock or a rarefaction wave that propagates towards the left (\leftarrow) or towards the right (\rightarrow) of the initial discontinuity, 1 and 2 are the known initial states with “state-vectors” consisting of fixed and independent values of the pressure, rest-mass density and velocity $\mathbf{U}_{1,2} \equiv (p, \rho, v)_{1,2}$. Similarly, 3 and 3' represent the new hydrodynamic states that form behind the two waves propagating in opposite directions. The two nonlinear waves \mathcal{W}_{\leftarrow} and $\mathcal{W}_{\rightarrow}$ are separated by a contact discontinuity \mathcal{C} across which the rest-mass density is discontinuous, but not the velocity nor the pressure, i.e. $\rho_3 \neq \rho_{3'}$, $p_3 = p_{3'}$, $v_3 = v_{3'}$. These three quantities fully describe the states of the fluid in the flow regions 3 and 3' behind the nonlinear waves. The formal solution of the Riemann problem consists then in determining the velocity, pressure and rest-mass density in the new states

3 and 3' as well as calculating, at any time $t > 0$, the positions of the waves separating the four states.

The solution of the Riemann problem attracted a wider interest when it was realized that its numerical solution could be implemented as building blocks in the construction of numerical Godunov-type methods for the accurate solution of the hydrodynamical equations [2]. In such methods, the computational domain is discretized and each interface between two adjacent grid-zones is used to construct the initial left and right states of a “local” Riemann problem. The evolution of the hydrodynamical equations is then obtained through the solution of the sequence of local Riemann problems set up at the interfaces between successive grid-zones and basically consists of determining the fluid pressure in regions 3 and 3' (see ref. [3] for a recent review).

The extension of the one-dimensional Riemann problem to relativistic fluid velocities has been performed by [4] for the “shock-tube” problem and by [5] for the general problem. Besides the obvious additional complications introduced by special relativity, the *one-dimensional* Riemann problem in relativistic hydrodynamics *does not* show qualitative differences from its Newtonian counterpart. In a recent paper [6], we have introduced a new approach to the solution of an exact relativistic one-dimensional Riemann problem which focuses on the relativistic invariant expression for the relative velocity between the two unperturbed initial states $(v_{12}^x)_0 \equiv [(v_1^x - v_2^x)/(1 - v_1^x v_2^x)]_0$, where we have assumed that the discontinuity is initially located on an $x = \text{const.}$ surface and where v^x represents the component of the 4-velocity normal to this surface. This new approach introduces great simplifications in the logical formulation of the Riemann problem and has been essential in revealing these new relativistic effects. For this reason we will briefly review it in what follows.

By construction, $(v_{12}^x)_0$ measures the relativistic jump of the fluid velocity normal to the discontinuity surface. Within this new approach, the solution to the relativistic Riemann problem is found after the pressure in the region between the two nonlinear waves has been calculated as the root of the

nonlinear equation [6]

$$v_{12}^x(p_3) - (v_{12}^x)_0 = 0. \quad (2)$$

The notation used in equation (2) needs an additional comment. It should be emphasized, in fact, that p_3 itself depends on the thermodynamical properties of the initial states so that $v_{12}^x = v_{12}^x(p_1, \rho_1, p_2, \rho_2)$. Note also that $v_{12}^x(p_3)$ does not depend on the value of the initial tangential velocities and has a functional form that is different for each of the three possible wave-patterns that might result from the decay of the initial discontinuity. In ref. [6] it was then shown that the wave-pattern produced in a one-dimensional relativistic Riemann problem by the decay of the discontinuity can be *predicted* from knowledge of the initial data. The possibility of predicting the wave-pattern from the initial conditions applies also to Newtonian hydrodynamics [7] and represents an important advantage since it allows one to deduce in advance which set of equations to use for the solution of the Riemann problem. From a mathematical point of view, the validity of the approach discussed in ref. [6] is based on the proof that the three branches of the function $v_{12}^x = v_{12}^x(p_3)$, corresponding to the three possible wave-patterns, are monotonically increasing with p_3 . Furthermore, it was shown that the three different branches always join smoothly through specific values of $v_{12}^x(p_3)$ denoted respectively as $(\tilde{v}_{12}^x)_{2S}$ and $(\tilde{v}_{12}^x)_{SR}$. (In ref. [6] another limiting value, $(\tilde{v}_{12}^x)_{2R}$, was found but this is not relevant in the present discussion and will not be considered here.)

Exploiting these properties, an improved exact Riemann solver can be built in which the comparison of $(v_{12}^x)_0$ with the relevant limiting values $(\tilde{v}_{12}^x)_{2S}$ and $(\tilde{v}_{12}^x)_{SR}$ constructed from the initial conditions allows to determine, prior to solving equation (2), both the wave-pattern produced and the functional form of $v_{12}^x(p_3)$ to be used in equation (2) [6]. In practice, this approach leads to a straightforward numerical implementation and a more efficient numerical algorithm with computational costs reduced by up to 30%.

In generic multidimensional flows, the Riemann problem can still be cast in terms of a planar discontinuity surface across which a normal flow with velocity v^x takes place and is responsible for the mass transfer. In general, however, the flow will also have components tangential to the discontinuity surface, which we will refer to as $v^t \equiv [(v^y)^2 + (v^z)^2]^{1/2}$. The latter can also be discontinuous across \mathcal{C} possibly leading to a Kelvin-Helmholtz instability there. In relativistic regimes, the tangential component cannot be removed by a single Lorentz boost and is constrained to satisfy $|v^t| < [1 - (v^x)^2]^{1/2}$.

A first study of a multidimensional relativistic Riemann problem involving two strong rarefactions was carried out in ref. [8] and has been extended to a more general treatment in ref. [9] where it was pointed out that the tangential velocities in multidimensional flows introduce differences between the Newtonian and the relativistic Riemann problems. In Newtonian hydrodynamics, in fact, the solution to the Riemann problem does not depend on the tangential component of the

flow. In relativistic hydrodynamics, on the other hand, the different regions of the flow are coupled, both in the velocities and in the specific enthalpy, through the Lorentz factors $W_i \equiv [1 - (v_i^x)^2 - (v_i^t)^2]^{-1/2}$, where $i = 1, 2$. This is an important difference whose consequences are much harder to assess.

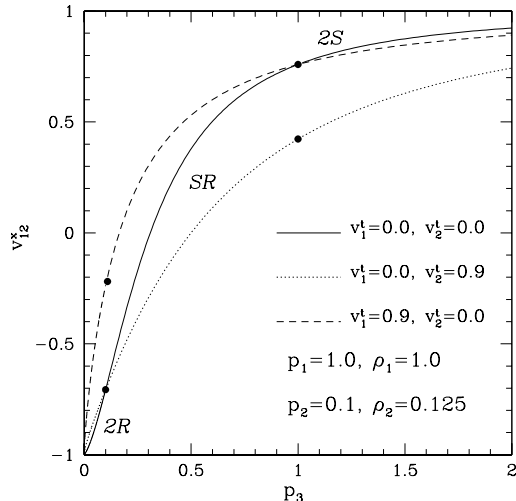


FIG. 1. Relative velocity as a function of the pressure in region 3. The continuous line refers to the case of zero tangential velocities while the dashed and dotted ones refer to cases in which the tangential velocities are nonzero (We use units in which $c = 1$). The filled circles represent the joins between the solutions consisting of two shock waves (2S), of one shock and one rarefaction wave (SR) and of two rarefaction waves (2R).

To discuss the *new* effects that emerge in a *multidimensional* and *relativistic* Riemann problem we have plotted in Fig. 1 the function v_{12}^x for different values of the pressure at the contact discontinuity p_3 . The curves shown refer to the case of zero tangential velocities (continuous line) and to the cases where the tangential velocities are nonzero (dashed and dotted lines), respectively (Note that the curves do not depend on the sign of v^t). In both cases the relative velocities are calculated for a perfect fluid with polytropic equation of state $p = k\rho^\gamma$, with a standard set of the initial values of pressure and rest-mass density [10], i.e. $p_1 = 1.0, p_2 = 0.1, \rho_1 = 1.0, \rho_2 = 0.125$ (we have here chosen $\gamma = 5/3$). The filled dots in each curve indicate the locations where the branches representing the three wave-patterns (2S, SR, and 2R) merge. The values of the relative normal-velocities where this happens are just the values of $(\tilde{v}_{12}^x)_{2S}$ and $(\tilde{v}_{12}^x)_{SR}$ mentioned above.

A rapid examination of Fig. 1 is sufficient to appreciate that the presence of tangential velocities can introduce new qualitative differences in a relativistic Riemann problem. When tangential velocities are present, in fact, the relative normal-velocity v_{12}^x is a function of p_3 but, through the coupling introduced by the Lorentz factors, also of v_1^t and v_2^t . This can introduce a *new relativistic effect* and *shift the solution from one wave-pattern to another*. To better appreciate this, let us

restrict attention to a simpler situation in which only one of the two initial tangential velocities is allowed to vary.

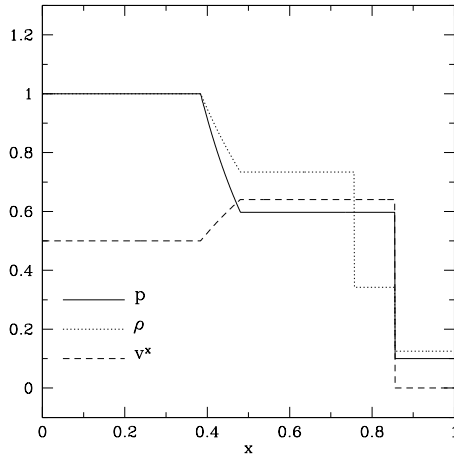


FIG. 2. Solution of the Riemann problem with initial conditions: $p_1 = 1.0, p_2 = 0.1, \rho_1 = 1.0, \rho_2 = 0.125$. The initial velocities are $v_1^t = 0.0 = v_2^t$ and $v_1^x = 0.5, v_2^x = 0.0$.

Suppose now that the normal velocities are chosen to be $v_1^x = 0.5, v_2^x = 0.0$, and that there are no tangential velocities. In this case, $(v_{12}^x)_0 = 0.5$ and Fig. 1 shows that the solution to the Riemann problem falls in the SR branch, hence producing a wave-pattern consisting of a shock and a rarefaction wave moving in opposite directions. This is presented in Fig. 2 which shows the solution of the Riemann problem at a time $t > 0$ for the pressure, the rest-mass density and the velocity. However, if we now maintain the *same* initial con-

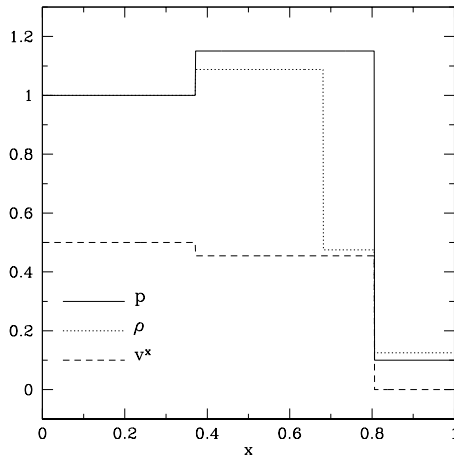


FIG. 3. As in Fig. 2 but with $v_1^t = 0.0, v_2^t = 0.9, v_1^x = 0.5, v_2^x = 0.0$.

ditions but allow for nonzero tangential velocities in state 2, Fig. 1 also shows that the solution to the Riemann problem can fall in the $2S$ branch (cf. dotted line), hence producing a wave-pattern consisting of two shock waves moving in opposite directions. This is presented in Fig. 3 which shows the solution of the same Riemann problem as in Fig. 2 but with

the initial tangential velocities being $v_1^t = 0.0$ and $v_2^t = 0.9$. Note that except for the tangential velocities, the solutions in Figs. 2 and 3 have the same initial state-vectors but different intermediate ones (i.e. p_3, ρ_3 , and v_3^x).

The Riemann problems shown in Figs. 2 and 3 are only two possible examples but they are useful ones since they show that through the coupling among the different states introduced by the Lorentz factors, a difference in the tangential velocities can produce a smooth transition from one wave-pattern to another while maintaining the initial states unmodified. Interestingly, this transition does not need to always produce a solution consisting of two shock waves.

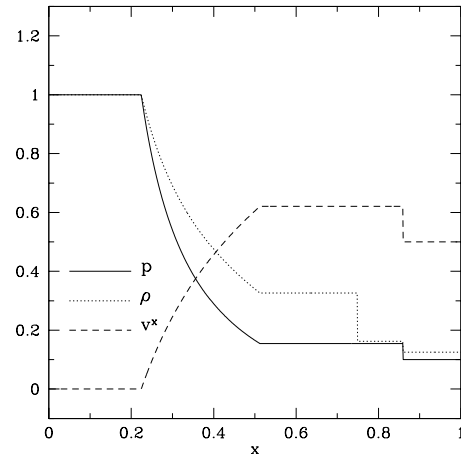


FIG. 4. As in Fig. 2 but with $v_1^t = 0.0 = v_2^t, v_1^x = 0.0, v_2^x = 0.5$.

Suppose, in fact, that the normal velocities are now chosen to be $v_1^x = 0.0, v_2^x = 0.5$. We can then repeat the considerations made above and start examining the wave-pattern produced when there are zero tangential velocities. In this new setup, $(v_{12}^x)_0 = -0.5$ and Fig. 1 shows that the solution to the Riemann problem still falls in the SR branch (cf. dashed line), with the corresponding solution at a time $t > 0$ being presented in Fig. 4. Note that the wave-patterns in Fig. 2 and 4 both consist of a shock and a rarefaction wave, but have alternate initial normal velocities.

When nonzero tangential velocities are now considered in state 1, Fig. 1 shows that $(v_{12}^x)_0$ can fall in the $2R$ branch, hence producing a wave-pattern consisting of two rarefaction waves moving in opposite directions. This is again shown in Fig. 5 where we have chosen initial tangential velocities $v_1^t = 0.9$ and $v_2^t = 0.0$. In this case too and except for the tangential velocities, the solutions in Figs. 4 and 5 have the same initial state-vectors but different intermediate ones.

As mentioned above, the appearance of these new relativistic effects is related to the behaviour of the function v_{12}^x for different values of the initial tangential velocities and in particular to how the three branches composing the curve change under variation of $v_{1,2}^t$. As a result, the occurrence of these effects can be recast into the study of the functional behaviour of the values of v_{12}^x delimiting the different branches when the

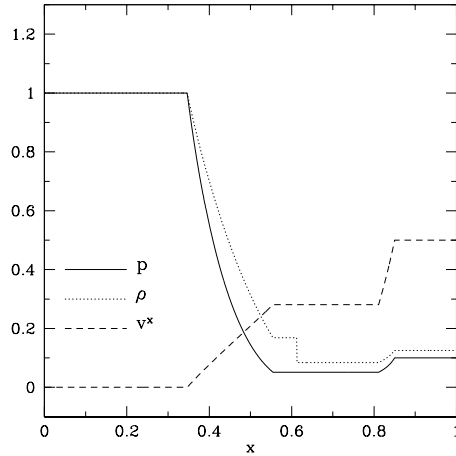


FIG. 5. As in Fig. 2 but with $v_1^t = 0.9$, $v_2^t = 0.0$, $v_1^x = 0.0$, $v_2^x = 0.5$.

tangential velocities are varied within the allowed ranges. A detailed mathematical treatment of this problem will be presented in a separate paper [11] but it is sufficient to point out in what follows the main results. Firstly, the dependence of the limiting values for the SR and $2S$ branches on the tangential velocities can be expressed as (cf. Fig. 1)

$$(\tilde{v}_{12}^x)_{SR} = (\tilde{v}_{12}^x)_{SR}(v_1^t), \quad (\tilde{v}_{12}^x)_{2S} = (\tilde{v}_{12}^x)_{2S}(v_2^t). \quad (3)$$

Secondly, these values converge to zero when the tangential velocities are allowed to reach their maximum values, i.e.

$$\lim_{W_1 \rightarrow \infty} (\tilde{v}_{12}^x)_{SR} = 0 = \lim_{W_2 \rightarrow \infty} (\tilde{v}_{12}^x)_{2S}. \quad (4)$$

Expressions (4) indicate that for tangential velocities assuming increasingly larger values, the SR branch of the v_{12}^x curve spans a progressively smaller interval of relative normal velocities. When the tangential velocities reach their asymptotic values, the SR branch reduces to a point. As a result, a wave-pattern consisting of a shock and a rarefaction wave is generically disfavoured by increasing tangential velocities.

The effects discussed so far have a purely special relativistic origin and might conflict with our physical intuition. However, a behaviour similar to the one reported here is found in the well-known relativistic transverse-Doppler effect, in which the wavelength of a photon received from a source moving at relativistic speeds changes also if the source has a velocity component orthogonal to the direction of emission of the photon [12]. In this case too, a Lorentz factor including the transverse velocity is responsible for the effect.

A couple of comments are worth mention. Firstly, there exists a set of initial conditions for which these new relativistic effects will not occur. These initial conditions are those of the classic ‘‘shock-tube’’ problem, in which $v_1^x = 0 = v_2^x$. In this case, in fact, $(\tilde{v}_{12}^x)_0 = 0$ and, because of the limits (4), the solution of the Riemann problem will be given by a wave-pattern consisting of a shock and a rarefaction wave, independently of

the values of the tangential velocities. Secondly, while the stability of shock fronts has been studied in the past (see [13] and references therein), little is still known about the stability properties of shock fronts across which the tangential velocities are discontinuous. It is plausible that a nonzero mass flux makes these fronts stable with respect to the Kelvin-Helmholtz instability, but more work needs to be done in the investigation of the stability of generic shocks fronts.

The results reported in this letter can be used in astrophysical scenarios, such as those involving relativistic jets or γ -ray bursts, in which nonlinear hydrodynamical waves with large Lorentz factors and complex multidimensional flows are expected [14]. Furthermore, both the approach to the solution of the Riemann problem and the new relativistic effects discussed here could be relevant in the implementation of special relativistic exact Riemann solvers in multidimensional codes solving the hydrodynamical equations in curved spacetimes [9,15].

It is a pleasure to thank J.C. Miller and J.A. Pons for useful discussions. Support for this research has been provided by the MIUR and by the EU Network Programme (Research Training Network Contract HPRN-CT-2000-00137).

-
- [1] R. Courant and K. O. Friedrichs, *Supersonic Flows and Shock Waves*, Springer-Verlag, New York (1976)
 - [2] S. K. Godunov, *Mat. Sb.*, **47**, 271 (1959); P. Colella and P. R. Woodward, *J. Comput. Phys.*, **54**, 174 (1984)
 - [3] J. M. Martí and E. Müller, *Living Reviews*, **3** (1999)
 - [4] K. W. Thompson, *J. Fluid Mech.*, **171**, 365 (1986)
 - [5] J. M. Martí and E. Müller, *J. Fluid Mech.*, **258**, 317 (1994)
 - [6] L. Rezzolla and O. Zanotti, *J. Fluid Mech.* **449**, 395 (2001)
 - [7] L. D. Landau and E. M. Lifshitz., *Fluid Mechanics (Second Edition)*, Pergamon Press (1987)
 - [8] S. A. E. G. Falle and S. S. Komissarov, *Mon. Not. Royal Astron. Soc.*, **278**, 586 (1996)
 - [9] J. A. Pons, J. M. Martí and E. Müller, *J. Fluid Mech.* **422**, 125 (2000)
 - [10] G. A. Sod, *J. Comp. Phys.*, **27**, 1 (1978)
 - [11] L. Rezzolla and O. Zanotti, *In preparation* (2002)
 - [12] W. Rindler, *Introduction to Special Relativity*, Clarendon Press, New York (1982)
 - [13] A. M. Anile and G. Russo, *Phys. of Fluids*, **29**, 2487 (1986); *ibidem* **30**, 1045 (1987)
 - [14] R. D. Blandford, *Prog. of Theor. Phys. Supp.*, **143**, in press (2002) P. Meszaros, *Annu. Rev. Astron. Astrophys.* **40** in press (2002)
 - [15] J. A. Pons, J. A. Font, J. M. Martí J. M. Ibañez and J. A. Miralles, *Astron. Astroph.* **339**, 638 (1998)